

## X-RAY AND EUV SPECTROSCOPY OF THE BOUNDARY LAYER EMISSION OF NONMAGNETIC CATAclySMIC VARIABLES

Christopher W. Mauche  
Lawrence Livermore National Laboratory,  
L-41, P.O. Box 808, Livermore, CA 94550, USA

### Abstract

*EUVE*, *ROSAT*, and *ASCA* observations of the boundary layer emission of nonmagnetic cataclysmic variables (CVs) are reviewed. *EUVE* spectra reveal that the effective temperature of the soft component of high- $\dot{M}$  nonmagnetic CVs is  $kT \sim 10\text{--}20$  eV and that its luminosity is  $\sim 0.1\text{--}0.5$  times the accretion disk luminosity. Although the EUV spectra are very complex and belie simple interpretation, the physical conditions of the boundary layer gas are constrained by emission lines of highly ionized Ne, Mg, Si, and Fe. *ROSAT* and *ASCA* spectra of the hard component of nonmagnetic CVs are satisfactorily but only phenomenologically described by multi-temperature thermal plasmas, and the constraints imposed on the physical conditions of this gas are limited by the relatively weak and blended lines. It is argued that significant progress in our understanding of the X-ray spectra of nonmagnetic CVs will come with future observations with *XMM*, *AXAF*, and *Astro-E*.

### 1. Introduction

In the standard theory of disk accretion in nonmagnetic cataclysmic variables, half of the gravitational potential energy of accreted material is dissipated in the disk, and half is dissipated in the boundary layer between the disk and the surface of the white dwarf. The luminosity of the boundary layer is  $L = GM_{\text{wd}}\dot{M}/2R_{\text{wd}} = 8 \times 10^{34} (M_{\text{wd}}/M_{\odot})(\dot{M}/10^{-8} M_{\odot}\text{yr}^{-1})(R_{\text{wd}}/5 \times 10^8 \text{ cm})^{-1} \text{ erg s}^{-1}$ , where  $M_{\text{wd}}$  is the mass of the white dwarf,  $R_{\text{wd}}$  is its radius, and  $\dot{M}$  is the mass-accretion rate. The temperature of the boundary layer is bounded from below by the blackbody temperature  $kT_{\text{low}} = k(GM_{\text{wd}}\dot{M}/8\pi\sigma R_{\text{wd}}^3)^{1/4} \sim 10$  eV and from above by the virial temperature  $kT_{\text{high}} = GM_{\text{wd}}\mu m_{\text{H}}/3R_{\text{wd}} \sim 60$  keV. The former applies in high- $\dot{M}$  systems (i.e., nova-like variables and dwarf novae in outburst) wherein the boundary layer is optically thick and the radiation is thermalized before escaping, and the latter applies in low- $\dot{M}$  systems (i.e., dwarf novae in quiescence) wherein the boundary layer is optically thin. However, even high- $\dot{M}$  systems have a high-energy component in their spectra due to the inevitable optically thin portion of the boundary layer. The physical conditions in the boundary layer are determined by radiation hydrodynamic processes which are too complex to model with fidelity, and depend on such unknowns as the rotation rate of the white dwarf and the nature and magnitude of the viscosity. Insight into the physical conditions in the boundary layer and its environs is afforded by spectroscopic studies in the extreme ultraviolet (EUV) through hard X-rays.

### 2. ROSAT Observations

*ROSAT* measured the X-ray spectra of CVs in an intermediate bandpass ( $E = 0.1\text{--}2.4$  keV) with moderate spectral resolution ( $E/\Delta E \sim 2.4$  at 1 keV). The broad picture of the X-ray spectra of  $\sim 120$  CVs is supplied by the *ROSAT* All-Sky Survey (Beuermann & Thomas

1993). Insufficient counts are typically collected to perform spectral fits, but useful diagnostics are provided by such hardness ratio diagrams as the total count rate versus the hardness ratio (hard – soft)/(hard + soft), where “soft” is the 0.07–0.40 keV flux and “hard” is the 0.40–2.40 keV flux. High- $\dot{M}$  AM Her-type CVs have hardness ratios  $< -0.5$  and, with the exception of SS Cyg in outburst, both low- and high- $\dot{M}$  nonmagnetic CVs have hardness ratios  $> -0.5$ . The soft spectra of high- $\dot{M}$  AM Her-type CVs is due to the expression of a large fraction of the accretion luminosity in a soft blackbody-like component having a temperature of a few tens of eV. The moderate-to-hard ratios of nonmagnetic CVs can be reproduced by a thermal brems spectrum with a temperature of a few to many keV. Absorption by a neutral hydrogen column drastically reduces the total count rate with only a modest variation in the hardness ratio for soft blackbody spectra, but under the same influence thermal brems spectra suffer large variations in the hardness ratio with only modest variations in the total count rate. Despite the many high- $\dot{M}$  nonmagnetic CVs observed during the All-Sky Survey, only SS Cyg in outburst clearly manifests a soft component in its spectrum (Ponman et al. 1995). When VW Hyi went into outburst, its hardness ratio remained constant while the total count rate *decreased* (Wheatley et al. 1996). The soft component of high- $\dot{M}$  nonmagnetic CVs is not detected because either its luminosity is significantly smaller than the high-temperature component, its temperature is too low to radiate soft X-rays, its flux is extinguished by photoelectric absorption in the ISM or a wind, or some combination of these factors. To distinguish among these alternatives, *EUVE* observations are required (§3).

Analysis of pointed *ROSAT* observations of nonmagnetic CVs is supplied by van Teeseling & Verbunt (1994), van Teeseling, Beuermann, & Verbunt (1996), Richman (1996), and references therein. The colors of nonmagnetic CVs can be reproduced by absorbed single-temperature thermal brems or optically thin thermal plasma spectra, but fits of the data to such models demonstrate that the spectra of nonmagnetic CVs are often more complex. van Teeseling & Verbunt found that acceptable fits could be obtained with either absorbed two-temperature optically thin thermal plasma spectra or absorbed single-temperature thermal brems spectra with a narrow emission line at  $\sim 1$  keV. Richman found that fits to absorbed thermal brems spectra produced excesses near 0.2 and 0.9 keV. Two-temperature absorbed thermal brems spectra did not significantly improve the fits, and although the addition of a narrow emission line at  $\sim 1$  keV did improve the fits, most of the reduction in  $\chi^2$  was due to the additional parameters in the model. Unfortunately, although *ROSAT* PSPC data is an improvement over *Einstein* IPC data in being able to tell that the spectra of nonmagnetic CVs are more complex than absorbed single-temperature models, the PSPC has neither the bandpass nor the spectral resolution required to distinguish between the alternatives. As such, the increase in complexity has not been accompanied by an increase in understanding. To accomplish this, the wider bandpass and higher spectral resolution of *ASCA* (§4), *XMM*, *AXAF*, and *Astro-E* are required (§5).

### 3. EUVE Observations

Observations in the EUV are needed to measure the soft component of the X-ray spectra of high- $\dot{M}$  CVs, but photoelectric absorption severely limits the effective bandpass and the number of sources that can be observed. Unit optical depth is reached for a hydrogen column density of  $N_{\text{H}} = 10^{18}$ ,  $10^{18.5}$ ,  $10^{19}$ ,  $10^{19.5}$ , and  $10^{20}$   $\text{cm}^{-2}$  at  $\lambda \sim 380$ , 235, 145, 95, and 65 Å, respectively. With the exception of VW Hyi, whose interstellar column density is  $\sim 6 \times 10^{17}$   $\text{cm}^{-2}$ , CVs have interstellar columns in excess of a couple times  $10^{19}$   $\text{cm}^{-2}$ . To make matters worse, high- $\dot{M}$  nonmagnetic CVs have winds which can absorb and scatter the boundary layer radiation. *EUVE* supplies high-resolution ( $\lambda/\Delta\lambda \sim 200$ ) spectra in the bandpass from 70 to 760 Å, but observations exist for only a few high- $\dot{M}$  nonmagnetic CVs: the nova-like variable IX Vel (van Teeseling et al. 1995) and the dwarf novae U Gem (§3.1), SS Cyg (§3.2), and VW Hyi (§3.3) in outburst.

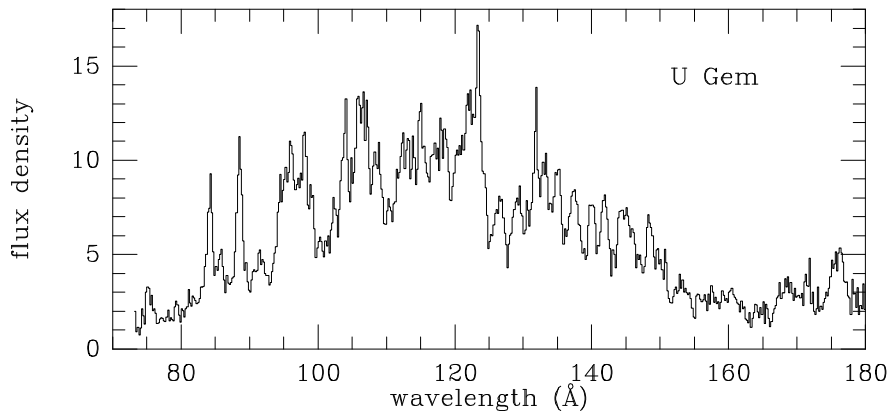


Fig. 1. *EUVE* spectrum of U Gem in outburst. Units of flux density are  $10^{-12}$  erg cm $^{-2}$  s $^{-1}$   $\text{\AA}^{-1}$ .

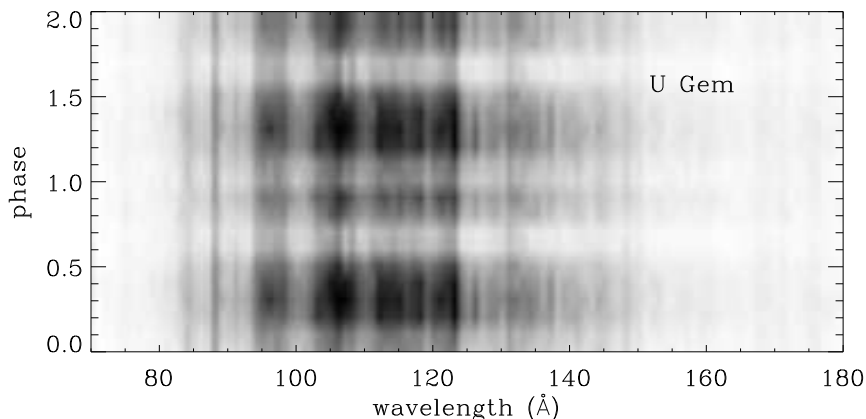


Fig. 2. *EUVE* spectra of U Gem in outburst as a function of binary phase for the ephemeris of Marsh et al. (1990). Note the partial eclipses at phases  $\phi \sim 0.1$  and  $0.65$  and the persistence through eclipse of many of the emission lines (e.g., Ne VIII 2s-2p  $\lambda 88.1$ ).

### 3.1. U Gem

The *EUVE* spectrum from the first interval of observations of U Gem in outburst is shown in Figure 1 (Long et al. 1996). The continuum is reasonably well described by a blackbody with an effective temperature  $T \sim 1.4 \times 10^5$  K (12 eV), a hydrogen column density  $N_{\text{H}} \sim 3 \times 10^{19}$  cm $^{-2}$ , a luminosity  $L \sim 4 \times 10^{34}$  ( $d/90$  pc) $^2$  erg s $^{-1}$ , and a fractional emitting area  $f \equiv L/4\pi R_{\text{wd}}^2 \sigma T^4 \sim 0.5$ . The boundary layer luminosity is  $\sim 0.5$  times the accretion disk luminosity, but U Gem in outburst would be a weak *ROSAT* source, since little flux is emitted shortward of  $\sim 80$   $\text{\AA}$  (0.16 keV).

Superposed on the continuum are emission lines of such species as Ne VI–VIII, Mg VI–VII, and Fe VII–X; species which dominate in collisionally ionized gas at  $T \sim 3\text{--}10 \times 10^5$  K or in gas photoionized by a blackbody at  $T \sim 2 \times 10^5$  K. The observed lines arise from ground-state transitions with substantial oscillator strengths, and the absence of lines from metastable levels combined with an estimate for the density of  $n_e \gtrsim 3 \times 10^{11}$  cm $^{-3}$  argues that the line-emitting gas is relatively cool and photoionized. That the line-emitting gas is also extended relative to the continuum is indicated by phase-resolved spectra. Figure 2 shows a gray-scale representation of

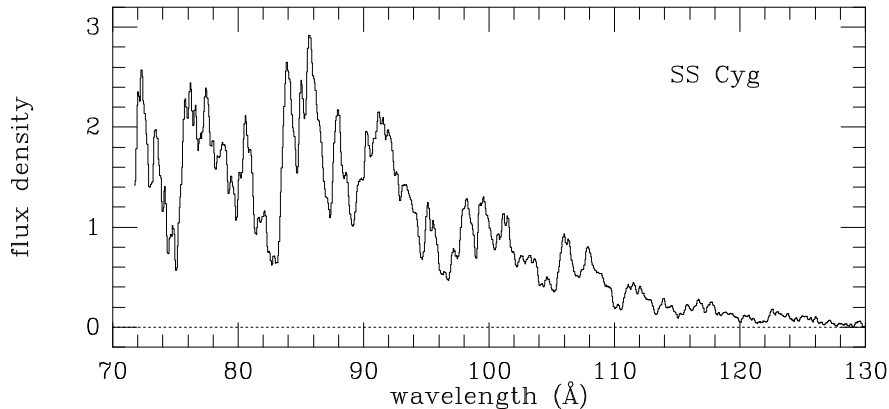


Fig. 3. *EUVE* spectrum of SS Cyg in outburst. Units of flux density are  $10^{-12}$  erg cm $^{-2}$  s $^{-1}$  Å $^{-1}$ .

the phase dependence of the EUV spectrum of U Gem. Partial eclipses occur at phases  $\phi \sim 0.1$  and 0.65, but the continuum is much more severely effected than the lines—note for example the persistence through eclipse of the Ne VIII 2s–2p line at 88.1 Å. These lines could arise in the wind or in a corona above the accretion disk.

### 3.2. SS Cyg

As shown in Figure 3, compared to U Gem, the *EUVE* spectrum of SS Cyg in outburst is hotter, more absorbed, less luminous, and less obviously separable into lines and continuum (Mauche, Raymond, & Mattei 1995). The spectrum is only crudely approximated by a blackbody with an effective temperature  $T \sim 2.3 \times 10^5$  K (20 eV), a hydrogen column density  $N_{\text{H}} \sim 7 \times 10^{19}$  cm $^{-2}$ , a luminosity  $L \sim 2 \times 10^{33} (d/75 \text{ pc})^2$  erg s $^{-1}$ , and a fractional emitting area  $f \sim 3 \times 10^{-3}$ . The boundary layer luminosity is only  $\lesssim 0.1$  times the accretion disk luminosity, but the higher effective temperature makes SS Cyg a bright *ROSAT* source. The peaks in the spectrum correspond to transitions of such species as Ne VI–VIII, Mg V–VIII, and Si IV–VII. These are roughly the same species as in the spectrum of U Gem and imply roughly the same conditions in the line-emitting gas. However, unlike U Gem, we have no constraint on the location or physical extent of this gas. Based on the morphology of the spectrum and the fact that the hydrogen column density is a factor of  $\sim 2$  higher than the interstellar value, the suspicion is that resonance scattering in the outflowing wind strongly modifies the intrinsic boundary layer spectrum, but a faithful model of the processes involved is beyond our current capabilities. To make matters worse, it is not clear that SS Cyg possesses a canonical boundary layer: the small effective area, the relatively high effective temperature, and the high-amplitude quasi-coherent oscillations in the EUV/soft X-ray flux suggest that the white dwarf in SS Cyg is weakly magnetic ( $B \sim 0.1$ –1 MG; Mauche 1996a).

### 3.3. VW Hyi

The comparatively cool and unabsorbed *EUVE* spectrum of VW Hyi in superoutburst is shown in Figure 4 (Mauche 1996b). A blackbody fails miserably to reproduce the overall spectral distribution, but the effective temperature must be  $T \lesssim 1.2 \times 10^5$  K (10 eV) and the hydrogen column density must be  $N_{\text{H}} \gtrsim 3 \times 10^{18}$  cm $^{-2}$ ; the bolometric luminosity is correspondingly uncertain, but the observed 80–420 Å luminosity is  $L \sim 8 \times 10^{32} (d/65 \text{ pc})^2$  erg s $^{-1}$ , which is  $\sim 0.05$  times the accretion disk luminosity. With little flux emitted shortward of  $\sim 100$  Å (0.12 keV), the boundary layer flux of VW Hyi in outburst is unobservable with *ROSAT*. If similar conditions apply in other high- $\dot{M}$  nonmagnetic CVs, the lack of detections of the soft

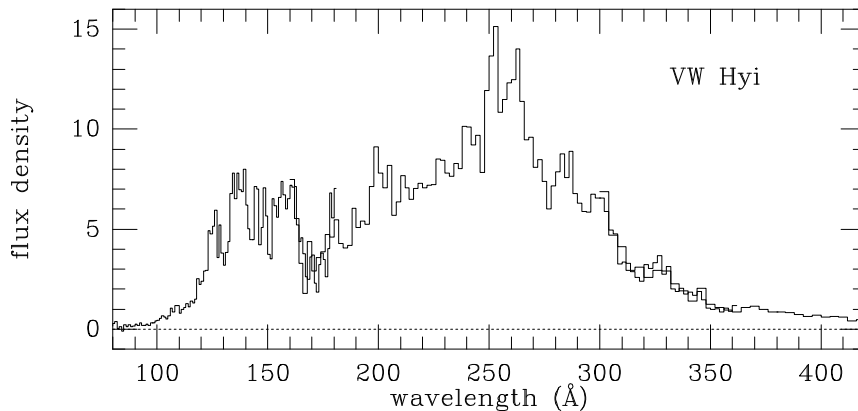


Fig. 4. *EUVE* spectrum of VW Hyi in superoutburst. Units of flux density are  $10^{-12}$  erg  $\text{cm}^{-2}$   $\text{s}^{-1}$   $\text{\AA}^{-1}$ .

component of such systems by *Einstein* and *ROSAT* is explained: *a la* Patterson & Raymond (1985), the boundary layer is simply too cool to radiate soft X-rays. But, we cannot simply move into the EUV to observe the boundary layer radiation: if the boundary layer temperature of VW Hyi were typical of other nearby CVs, the boundary layer flux would be unobservable even with *EUVE*: at  $N_{\text{H}} = 3 \times 10^{19}$   $\text{cm}^{-2}$ , the optical depth is 1.1 at 100  $\text{\AA}$ , 3.2 at 150  $\text{\AA}$ , 6.5 at 200  $\text{\AA}$ .

#### 4. ASCA Observations

*ASCA* has to date observed relatively few nonmagnetic CVs. SS Cyg was serendipitously observed in outburst during the PV phase (Nousek et al. 1994); VW Hyi (Mauche & Raymond 1994) and U Gem (Szkody et al. 1996) were observed in quiescence; and observations of about a dozen other CVs have been obtained, but to date none have been published. *ASCA* observations of Z Cam in outburst were obtained simultaneously with *HUT* UV and far-UV spectra in 1995 March. In a preliminary fit performed by M. Ishida, the SIS data are satisfactorily modeled by a two-temperature optically thin thermal plasma spectrum with  $kT \sim 0.8$  and 7 keV. Nousek et al. (1994) fit the *ASCA* SIS and GIS data for SS Cyg in outburst with three components: a two-temperature optically thin thermal plasma spectrum with  $kT \sim 0.8$  and 3.5 keV, plus a thermal brems spectrum with  $kT \sim 18$  keV. But, perhaps not surprising, it is now clear and that these two- and three-temperature fits are not unique descriptions of the data. Kitamura et al. (1997) fit the SS Cyg data with a three-temperature optically thin thermal plasma spectrum with  $kT \sim 0.3$ , 1, and 8 keV. Done & Osborne (1997) fit the same data with the spectrum of an optically thin thermal plasma with a continuous distribution of temperatures. Both groups now find a component of the Fe K line at  $\sim 6.47$  keV, indicating fluorescence from a photoionized plasma at  $\log \xi \lesssim 2.4$  and  $T \lesssim 2.5 \times 10^5$  K ( $kT \lesssim 22$  eV). This important result implies that the hot gas is in close proximity to relatively cold material such as the optically thick boundary layer, white dwarf, and/or accretion disk.

In both Z Cam and SS Cyg in outburst, the low-temperature component produces strong line emission from He-like Si (1.86 keV), S (2.46 keV), and Ar (3.14 keV), but these lines are strongly veiled by the continuum of the high-temperature component(s). The high-temperature component itself produces relatively weak lines of H-like Mg (1.47 keV), Si (2.01 keV), and S (2.62 keV), and these lines are themselves veiled by the brems component in the model of Nousek et al. The lines which are prominent in the *net* spectra are the Fe K blend at  $\sim 6.7$  keV and the Fe L complex at  $\sim 1$  keV. Whereas it is possible with the energy resolution

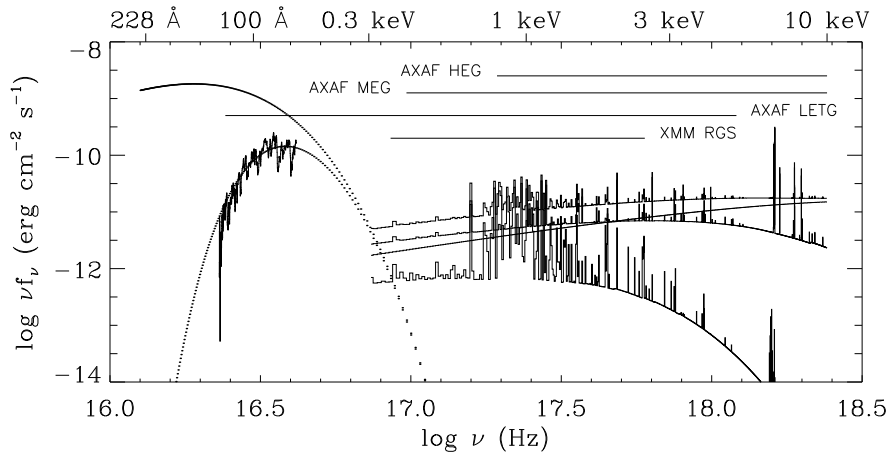


Fig. 5. Broad-band X-ray spectrum of SS Cyg in outburst. The horizontal lines indicate the wavelength/energy ranges of the *XMM* RGS and the *AXAF* LETG, MEG, and HEG.

of the *ASCA* SIS detector ( $E/\Delta E \sim 50$  at 6 keV) to resolve the Fe K line into its various components, nothing can be done with the forest of lines in the Fe L complex which dominate the spectrum from  $\sim 0.8$  to 1.2 keV.

## 5. The Future

While significant progress in our understanding of the X-ray spectra of nonmagnetic CVs has and will continue to be made with the growing list of sources observed by *ASCA*, it is not too soon to consider the improvements possible with the next generation of X-ray observatories. To demonstrate the case for one high- $\dot{M}$  CV, a montage broad-band X-ray spectrum of SS Cyg in outburst is shown in Figure 5. The figure shows the *EUVE* data on the left and the various components of the model of Nousek et al. for the *ASCA* data on the right. The dotted curves are the spectra of a 20 eV blackbody with and without absorption by  $N_{\text{H}} = 7 \times 10^{19} \text{ cm}^{-2}$ . The optically thick portion of the boundary layer forms a (not so) “big blue bump” in the EUV/soft X-ray waveband. This component will be observable (only) with the *AXAF* LETG with  $\sim 5$  times the effective area and  $\sim 5$  times the spectral resolution of the *EUVE* SW spectrometer. The Fe L forest is covered by the *XMM* RGS with comparable effective area and  $\sim 20$  times the spectral resolution of the *ASCA* SIS, and by the *AXAF* gratings with lower effective areas but  $\sim 30$ – $60$  times the spectral resolution. At the Fe K line, the *Astro-E* XRS has  $\sim 6$  times the effective area and  $\sim 10$  times the spectral resolution of the *ASCA* SIS. The *AXAF* LETG will extend the coverage of the soft component of the boundary layer into the soft X-ray waveband, supplying both the shape of the continuum to help constrain the bolometric luminosity, and additional spectral information to constrain the physical conditions in the optically thick portion of the boundary layer and the spectral formation processes responsible for its spectrum. The physical conditions of the optically thin portion of the boundary layer are constrained by observations with the other instruments. The *XMM* RGS and *AXAF* MEG and HEG will resolve the Fe L forest into its trees. These same instruments supply the highest spectral resolution for the K-shell transitions of N through K, while Ca through Fe and beyond are studied best with the *Astro-E* XRS. We expect to be able to derive the differential emission measure of the optically thin gas, its density, and excitation mechanism (collisional vs. photoionization). Where photoionization applies, the spatial distribution of the gas will be constrained by the ionization parameter  $\xi = L/nR^2$ .

The author is pleased to acknowledge D. Liedahl and J. Raymond for kindly reading and commenting on a draft of this manuscript and M. Ishida for the preliminary analysis of the *ASCA* observation of Z Cam. This work was performed under the auspices of the U.S. Department of Energy by Lawrence Livermore National Laboratory under contract No. W-7405-Eng-48.

## 6. References

1. Beuermann, K., & Thomas, H.-C. 1993, *Adv. Space Res.*, **13**, #12, 115.
2. Done, C., & Osborne, J. P. 1997, these proceedings.
3. Kitamura, H., Makishima, K., Matsuzaki, K., Ishida, M., & Fujimoto, R. 1997, these proceedings.
4. Long, K. S., Mauche, C. W., Raymond, J. C., Szkody, P., & Mattei, J. A. 1996, *ApJ*, **469**, 841.
5. Marsh, T. R., Horne, K., Schlegel, E. M., Honeycutt, R. K., & Kaitchuck, R. H. 1990, *ApJ*, **364**, 637.
6. Mauche, C. W. 1996a, *ApJ*, **463**, L87.
7. Mauche, C. W. 1996b, in *Cataclysmic Variables and Related Objects*, ed. A. Evans & J. H. Wood (Dordrecht: Kluwer), 243.
8. Mauche, C. W., & Raymond, J. C. 1994, in *New Horizon of X-ray Astronomy — First Results from ASCA*, ed. F. Makino & T. Ohashi (Tokyo: Universal Academy Press), 399.
9. Mauche, C. W., Raymond, J. C., & Mattei, J. A. 1995, *ApJ*, **446**, 842.
10. Nousek, J. A., et al. 1994, *ApJ*, **436**, L19.
11. Patterson, J., & Raymond, J. C. 1985, *ApJ*, **292**, 535.
12. Ponman, T. J., et al. 1995, *MNRAS*, **276**, 495.
13. Richman, H. R. 1996, *ApJ*, **462**, 404.
14. Szkody, P., Long, K. S., Sion, E. M., & Raymond, J. C. 1996, *ApJ*, **469**, 834.
15. van Teeseling, A., Beuermann, K., & Verbunt, F. 1996, *A&A*, **315**, 467.
16. van Teeseling, A., Drake, J. J., Drew, J. E., Hoare, M. G., & Verbunt, F. 1995, *A&A*, **300**, 808.
17. van Teeseling, A., & Verbunt, F. 1994, *A&A*, **292**, 519.
18. Wheatley, P. J., et al. 1996, *A&A*, **307**, 137.